

## **FHWA RESEARCH PROGRAM ON LIGHTWEIGHT HIGH-PERFORMANCE CONCRETE – SHEAR PERFORMANCE OF PRESTRESSED GIRDERS**

**Gary G. Greene, Jr., PhD, PE, PSI, McLean, VA**  
**Benjamin A. Graybeal, PhD, PE, FHWA, McLean, VA**

### **ABSTRACT**

*As part of a larger study focusing on the structural performance of lightweight high-performance concrete (LWHPC), researchers at the U.S. Federal Highway Administration fabricated 15 precast, prestressed LWHPC bridge girders in order to evaluate the shear performance of this type of concrete. The paper describes the overall scope of the research, test procedures, and preliminary results of 30 girder tests on the AASHTO Type II and AASHTO/PCI BT-54 girders. These tests are significant due to the lack of shear strength test data for this type of concrete.*

*Three different concrete mix designs were used in the girders. The mix designs included partial replacement of the coarse aggregate with lightweight aggregate, resulting in concrete equilibrium densities in the range between conventional lightweight and normal weight concrete. Variables investigated included the amount of shear reinforcement, lightweight aggregate source, girder depth, and the use of straight or draped strands. The cylinder compressive strengths of the girders at the time of test ranged from 8.8 to 11.9 ksi.*

*The maximum applied shear in all 30 tests was greater than the predicted shear resistance, with 10 of those tests ultimately concluding at shear failure. The mean experimental to predicted shear strength ratio for the tests ending in shear failure was 1.32. The shear resistance was predicted using the sectional design model of the AASHTO LRFD Bridge Design Specifications without including any modifications related to the use of lightweight concrete.*

**Keywords:** Bridge girder, Lightweight concrete, High-performance concrete, Prestressed concrete, Specified density concrete, Shear strength

## **INTRODUCTION**

The American Association of State Highway and Transportation Officials (AASHTO) Load and Resistance Factor Design (LRFD) Specifications from 2004 and earlier limited the design concrete compressive strength used in design to 10 ksi<sup>1</sup>. National Cooperative Highway Research Program (NCHRP) Project 12-56 was aimed at evaluating the use of design strengths above 10 ksi for shear resistance<sup>2</sup>. However, the project's scope was limited to normal weight concrete. More recently, NCHRP Project 18-15 has focused on high-strength lightweight concrete, including an investigation on the shear strength of bridge girders. While the results of this study have not yet been published, the scope of the research is limited to "traditional" lightweight concrete with a unit weight less than 125 pcf. Additional research is needed on the shear strength of high-strength concrete having a unit weight between traditional lightweight and normal weight concrete as defined in the AASHTO LRFD Specifications. This range of unit weight from 120 to 135 pcf is commonly known as "specified density" concrete.

Lightweight aggregate is known to have a lower tensile strength than normal weight aggregate<sup>3</sup>. Previous research investigations on the shear performance of small normal-strength, non-prestressed beams have shown that the shear strength of girders without web reinforcement is less for lightweight aggregate concrete than for normal weight concrete<sup>4</sup>. Prior research has not specifically addressed how the tensile strength of lightweight aggregate will affect the shear performance in prestressed girders made from specified density LWHPC.

Only minimal research has been performed on large, high-strength, prestressed girders using traditional lightweight concrete as defined by the AASHTO LRFD Specifications<sup>5-7</sup>. Correspondingly, no shear tests were found in the literature on similar specified density girders. The results of this research program should facilitate the development of proposals to modify the shear provisions of the AASHTO LRFD Specifications as they relate to the use of lightweight aggregate.

## **RESEARCH SIGNIFICANCE**

This paper gives the preliminary results of an extensive study on the shear performance of prestressed girders made from specified density LWHPC. The inclusion of specified density concrete in the AASHTO LRFD Specifications would allow for the use of intermediate density concretes, thus potentially facilitating greater design efficiency and/or reducing shipping/erection costs by allowing a girder to be designed with a unit weight slightly less than normal weight concrete.

## **AASHTO APPROACH**

The shear provisions of the current AASHTO LRFD Specifications<sup>8</sup> account for lightweight concrete by using a modification factor in specific articles anywhere there is

a  $\sqrt{f'_c}$ . Article 5.8.2.2 states that when the splitting tensile strength is specified ( $f_{ct}$ ) that  $\sqrt{f'_c}$  in Articles 5.8.2 and 5.8.3 should be replaced by  $4.7f_{ct}$ , but not greater than  $\sqrt{f'_c}$ . This is equivalent to the modification factor for lightweight concrete ( $\lambda$ ) in the ACI 318-08 Building Code<sup>9</sup>, where  $\lambda$  is equal to  $f_{ct}/6.7\sqrt{f'_c}$ , but not greater than unity. Where  $f_{ct}$  is not specified,  $\sqrt{f'_c}$  is reduced by using a multiplier of 0.75 for an all lightweight concrete and by 0.85 for a sand lightweight concrete. The modification factor for lightweight concrete affects the requirements for the minimum transverse reinforcement given in Article 5.8.2.5, the component of the shear resistance that relies on the tensile strength of concrete ( $V_c$  term) given in Article 5.8.3.3, the nominal shear resistance provided by concrete when inclined cracking results from combined shear and moment ( $V_{ci}$  term) and from excessive principal tensions in the web ( $V_{cw}$  term) given in Article 5.8.3.4.3, and the inclination angle of diagonal compression ( $\theta$ ) used to calculate the shear resistance using the Simplified Procedure of Article 5.8.3.4.3.

Lightweight aggregate concrete might also affect the maximum shear resistance given in Article 5.8.3.3 or the limit given in 5.8.3.2 for the use of the sectional design method. The maximum limit on the shear resistance of  $0.25f'_c$  was investigated in NCHRP Project 12-56 for high-strength normal weight concrete. The  $0.25f'_c$  was derived from the Modified Compression Field Theory<sup>10</sup> (MCFT), a sectional analysis that assumes a uniform field of diagonal compression. An outcome of the NCHRP project was to limit applicability of the sectional analysis given in Article 5.8.3.3 to a maximum shear stress of  $0.18f'_c$  near a support<sup>11</sup>. The  $0.18f'_c$  limit was provided to limit the compressive stresses that funnel to a support, and allow the stirrups to yield before local crushing in the web near the support. The AASHTO LRFD Specifications require shear stresses higher than  $0.18f'_c$  to be designed using a strut-and-tie model as described in Article 5.6.3.

Design of concrete members with lightweight aggregate in the AASHTO LRFD Specifications is also affected by the resistance factor ( $\phi$ ). The  $\phi$  factor is used to reduce the calculated shear resistance to account for variations in material properties, uncertainty in the calculation method, and differences in the performance of shear tests on normal weight and lightweight members. The current AASHTO LRFD Specifications prescribe a  $\phi$  of 0.90 and 0.70 for the calculated shear resistance of normal weight and lightweight members, respectively. The  $\phi$  for shear resistance of LWHPC members is beyond the scope of this paper.

The 30 shear tests that are a part of this study examine the applicability of the current shear provisions in the AASHTO LRFD Specifications for high-strength, specified density concrete girders. These tests are a part of a larger study focusing on the structural performance LWHPC being performed by researchers at the Turner-Fairbank Highway Research Center (TFHRC) which is a part of the U.S. Federal Highway Administration (FHWA).

## EXPERIMENTAL PROGRAM

The experimental program consisted of 30 tests on 15 prestressed concrete girders made using three different specified density LWHPC mixes. The main variables investigated in the program included the amount of shear reinforcement, lightweight aggregate source, girder depth, and the use of straight or draped strands. The rest of this section will describe the concrete mix designs, the design of the girder specimens, the test setup, the instrumentation, and the test procedure.

### GIRDER MIX DESIGN

One of the objectives of this research project was to use lightweight aggregate sources that were geographically distributed across the United States. The Expanded Shale, Clay, and Slate Institute (ESCSI) assisted FHWA in obtaining specified density mixes that had been used in production. The mix designs selected are shown in Table 1 and used partial replacement of the coarse aggregate with lightweight aggregate to achieve their unit density. The lightweight aggregates in the mixes were Haydite, an expanded shale from Ohio, Stalite, an expanded slate from North Carolina, and Utelite, an expanded shale from Utah. The normal weight coarse aggregate was No. 67 Nova Scotia granite. Natural river sand was used as the fine aggregate. Type III portland cement was used to obtain the high early strengths typically required in high-strength precast girders. Admixtures included a water reducer, an air entrainer, and a high range water reducer. The water-to-cementitious materials ratio ranged from 0.31 to 0.36. The mean unit weight of the concrete mixes based on 28-day cylinders was 132 pcf for Haydite, 125 pcf for Stalite, and 130 pcf for Utelite.

Table 1 Girder Concrete Mix Designs

	unit	Stalite Mix	Haydite Mix	Utelite Mix
Design 28-Day Strength	psi	10,000	6,000	7,000
Design Release Strength	psi	7,500	3,500	4,200
Target Unit Weight	pcf	126	130	126
Lightweight Coarse Aggregate	lb	880	800	740
Normal Weight Coarse Aggregate	lb	250	520	385
Normal Weight Sand	lb	1,221	1,185	1,267
Class F Fly Ash	lb	-	-	150
Type III Portland Cement	lb	800	750	600
Water	lb	250	267	259
Water Reducer	oz	19	19	19
Air Entrainment	oz	2	2	2
High Range Water Reducer	oz	34	34	34
Water / Cementitious Materials Ratio		0.31	0.36	0.34

The girders were fabricated at the Standard Concrete Products (SCP) plant in Mobile, Alabama. The fabricator was asked to prescriptively produce the concrete mixes, without

trying to adjust them for target strengths or unit weight. This was intended to remove batch-to-batch variations as a variable in the study. The lightweight aggregates were stored in three piles at the plant and watered continuously using a sprinkler on each pile. After casting, the girders were stored on site before being shipped to TFHRC in McLean, Virginia. At TFHRC, 8 inch thick normal weight concrete decks were cast on the girders with dimensions and reinforcement as shown in Fig. 1 and Fig. 2. The concrete used in the decks had a specified compressive strength of 4 ksi.

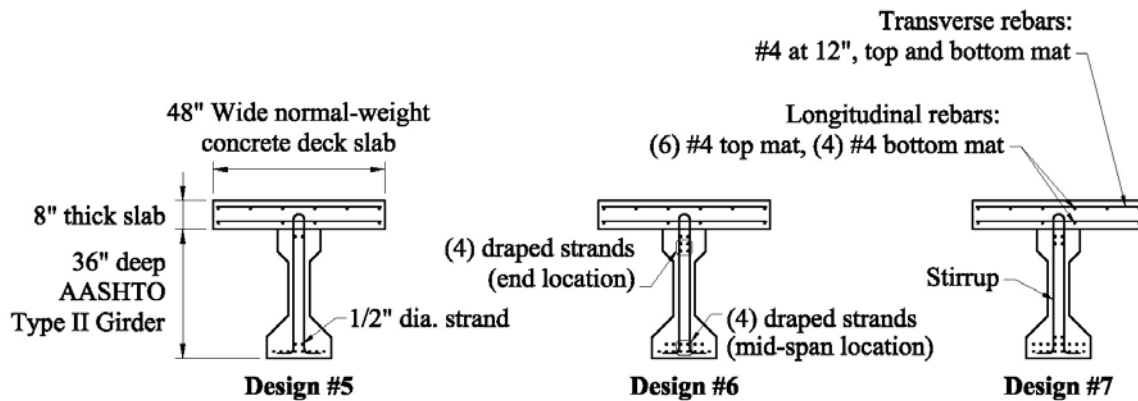


Fig. 1 AASHTO Type II Girder Cross Sections

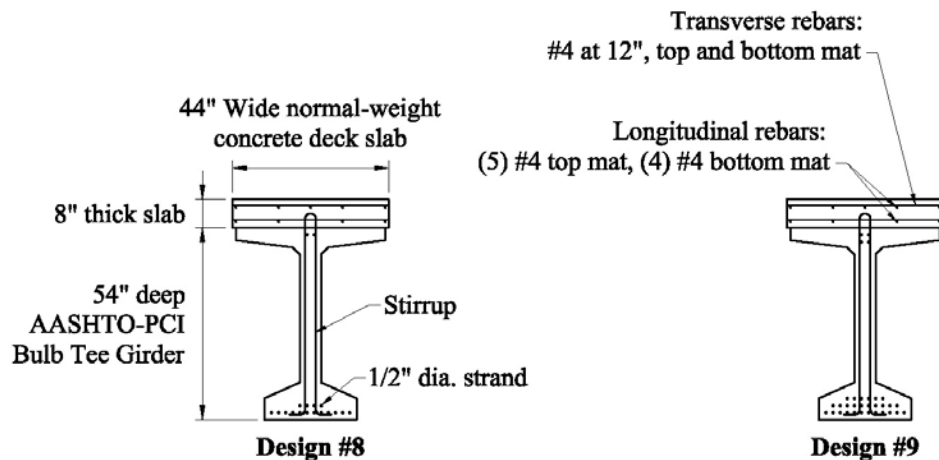


Fig. 2 AASHTO/PCI BT-54 Girder Cross Sections

## GIRDER DESIGN

The shear test girders were designed as part of a larger study that included the transfer and development length of prestressing strands in specific density LWHPC. A total of nine different girder designs were used in the overall research program. The first four designs were AASHTO Type II girders what were tested to failure to evaluate development length of prestressing strand. Girder Designs 5-9 were for the evaluation of shear performance.

Girder Designs 5-7 were Type II girders. The amount of shear reinforcement (stirrups) in the test regions near the live (L) and dead (D) ends of the girder was varied. The end of

the girder closer to the prestressing bed bulkhead where the strands were jacked is known as the live end, and the end towards the bulkhead with the stationary anchorage is known as the dead end. The design details for each girder end are shown in Table 2 and a sketch of the cross section is shown in Fig. 1. The dead end of Girder Design 5 (5D) was designed to have the minimum amount of shear reinforcement allowed by the AASHTO LRFD Specifications at nearly the maximum spacing. The dead end of Girder Design 7 (7D) was designed to have a ratio of shear stress to concrete compressive stress ( $v_u/f'_c$ ) near the limit of 0.18 given in the AASHTO LRFD Specifications for the applicability of the sectional design method. Girder Design 6 had draped strands and an amount of shear reinforcement between the amounts used in girder designs 5 and 7.

Table 2 Design Details of the AASHTO Type II Girders

Girder End	$d_v$ , inch	Design $v_u / f'_c$	No. of Strand		Stirrups		$\rho_v f_y$ , psi
			Bottom	Top	Size, No.	Spacing, inch	
5D	35.0	0.068	10-straight	2	3	22	120
5L	35.0	0.075	10-straight	2	3	15	176
6D	31.7	0.088	10-straight + 4-drape	2	4	15	320
6L	31.7	0.096	10-straight + 4-drape	2	4	12	400
7L	32.8	0.12	18-straight	4	4	12	400
7D	32.8	0.15	18-straight	4	4	8	600

Notes: Specimen name of form #%, where: # is girder design; % is D for dead end or L for live end; and assumed  $f'_c$  for design at test of 10,000 psi

The last two designs were 54-inch deep AASHTO/PCI Bulb Tee girders (BT-54). The design details for the live and dead ends of the girders are shown in Table 3 and a sketch of the cross section is shown in Fig. 2. The amount of shear reinforcement in girder designs 8 and 9 was designed to give similar  $v_u/f'_c$  ratios as girder designs 5 and 7, respectively. This was done investigate the effect that girder depth has on shear strength which is commonly known as “size effect”.

The end of each girder had additional reinforcement as required by the AASHTO LRFD Specifications. No. 6 rebar was added between the strands in the bottom flange to satisfy the requirements of Article 5.8.3.5 for additional longitudinal reinforcement. Additional transverse reinforcement (as stirrups) was provided as splitting resistance in the pretensioned anchorage zone per Article 5.10.10.1. Confinement reinforcement was provided around the strands to satisfy Article 5.10.10.2.

Table 3 Design Details of the AASHTO/PCI BT-54 Girders

Girder End	$d_v$ , inch	Design $v_u / f'_c$	No. of Strand		Stirrups		$\rho_v f_y$ , psi
			Bottom	Top	Size	Spacing, inch	
8D	51.6	0.068	16-straight	2	3	22	120
8L	51.6	0.076	16-straight	2	3	14	189
9L	47.5	0.14	28-straight	4	4	10	480
9D	47.49	0.15	28-straight	4	4	8	600

Notes: Specimen name of form #%, where: # is girder design; % is D for dead end or L for live end; and assumed  $f'_c$  for design at test of 10,000 psi

The girders were designed with an amount of flexural reinforcement that was intended to ensure that a shear failure would occur prior to a flexural failure. An  $f'_c$  of 10 ksi was assumed for all girders and no modification of the shear resistance for lightweight concrete was used. The first three shear tests (A7L, B7L, and C7L) reached a much higher applied shear than expected and there was concern that subsequent tests would not experience shear failures unless the flexural resistance of the girders was increased. Glass fiber reinforced polymer (FRP) was bonded to the lower surface and sides of the bottom flange on many of the remaining shear tests in order to increase the girder flexural capacity. The FRP layers were kept as far from the critical section for shear as possible in order to avoid increasing the girder's shear resistance due to the increased longitudinal restraint provided by the FRP. The effect that longitudinal strain has on shear resistance will be described later in this paper.

## TEST SETUP

A photograph of the test setup is shown in Fig. 3. Before a test, the girder was supported by a roller at the end being subjected to high shear, and by a "loading support" at the other end of the span. The loading support consisted of a roller between two grooved plates supported by a large hydraulic jack. The load in the jack was controlled by a closed-loop servo-valve system. The feedback for the closed loop system was provided by a loadcell with a 300 kip capacity mounted between the jack and roller and by an LVDT with a 10-inch stroke. The loading was applied by specifying the jack force in "load-control" or by specifying the jack travel in "displacement-control". When the jack applied load to the girder, it was reacted by a heavy load frame through a spherical bearing (not shown in Fig. 3), a spreader beam, and two pairs of 300 kip loadcells on the deck that applied the reaction force into the girder. The locations of the loadcell pairs on the deck are referred to as the "deck reaction points" in this paper.

The distance between the centerline of the roller support and the closest deck reaction point is the shear span ( $a$ ). The "test region" for each girder end was defined as the portion of the girder along the shear span. The ratio of the shear span to the effective girder depth for shear ( $d_v$ ) is given in Table 4 and Table 5 for the Type II and BT-54 girders, respectively. An  $a/d_v$  ratio of less than 2.5-3.0 has been shown to increase the shear strength of a girder<sup>4,7</sup>. The target  $a/d_v$  ratio was 3.0, however the girders were tested over a range of  $a/d_v$  ratios from 2.6 to 3.4. The shear span was adjusted from test

to test during the first seven tests on Type II girders in order to force a shear failure. However, starting with the seventh test, the shear span was left constant so variations in the  $a/d_v$  ratio in subsequent tests can be attributed to the differences in the calculated  $d_v$  for different girder designs.

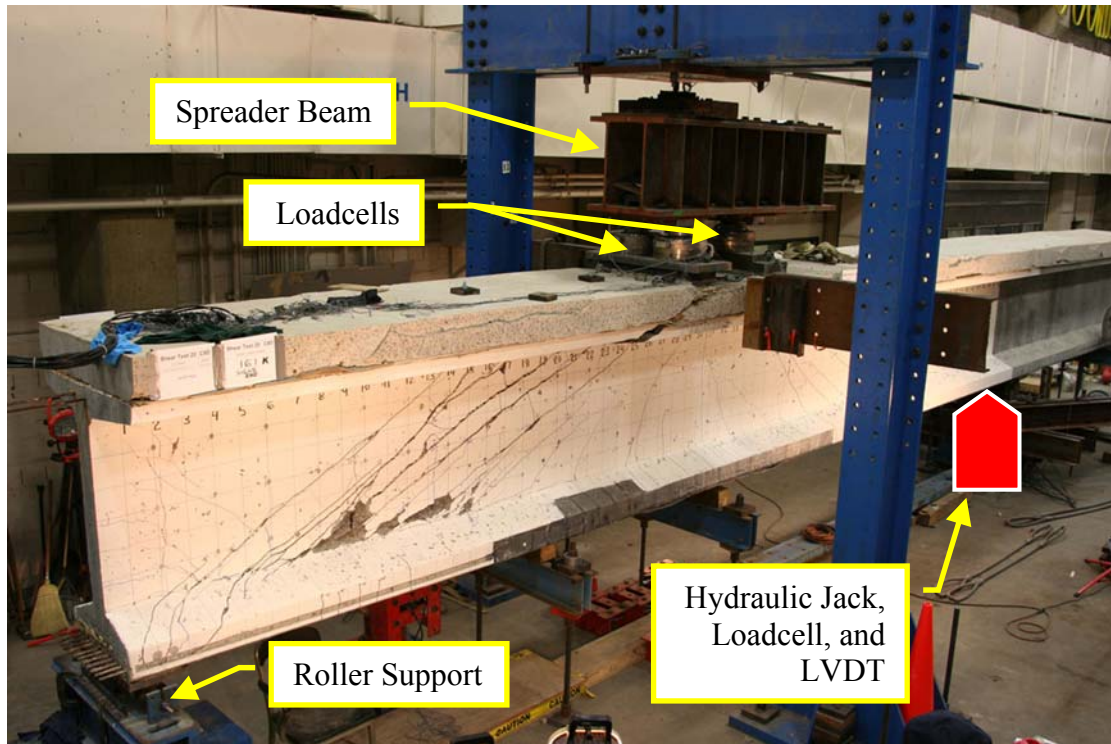


Fig. 3 Test Setup on Girder End C8D (Shear Failure Type SW)

## INSTRUMENTATION

The shear tests were extensively instrumented to measure applied forces, reaction forces, girder deformations, girder curvature, reinforcement strain, average concrete strain in the web, strand end slip, and concrete deck strain. The electronic instruments were connected to a data acquisition system that recorded data at a rate of 0.1 Hz.

Vertical deflections were measured using string potentiometers attached to the bottom flange directly below the deck reaction points. Vertical and horizontal deflections were measured using string potentiometers attached to the bottom flange directly over the loading support. These string potentiometers indirectly measured the deflection of the girder at the deck reaction points. Girder deflection was directly measured at the deck reaction points using a taut-line system consisting of a weighted wire passing by pairs of rulers and mirrors attached to the top flange directly below the deck reaction points. The mirrors were used to correct for parallax before reading the deflection to the nearest 1/128 inch on the rulers.



Table 4 Summary of Test Results – AASHTO Type II Girders

Test	a / d <sub>v</sub>	V <sub>test</sub> (kips)	Failure Modes	FRP	Stirrup Strain		LRFD (kips)	$\frac{V_{test}}{V_{LRFD}}$
					Max.	No. > 3 $\epsilon_y$		
A5D	2.57	219	FD	No	5.0 $\epsilon_y$	1	142	1.55
B5D	3.09	200	FF	Yes	5.0 $\epsilon_y$	2	142	1.41
C5D	3.09	206	FF	Yes	5.0 $\epsilon_y$	4	142	1.45
A5L	3.09	211	FF	Yes	5.0 $\epsilon_y$	6	154	1.37
B5L	3.09	201	FF	Yes	5.0 $\epsilon_y$	4	154	1.30
C5L	3.09	211	FF	Yes	5.0 $\epsilon_y$	3	154	1.37
A6D	3.41	205	FD	No	1.1 $\epsilon_y$	0	182	1.13
B6D	3.41	206	FD	No	1.0 $\epsilon_y$	0	182	1.13
C6D	3.41	207	FD	No	5.0 $\epsilon_y$	1	182	1.14
A6L	3.41	241	FF	Yes	4.9 $\epsilon_y$	1	195	1.24
B6L	3.41	244	FF	Yes	1.9 $\epsilon_y$	0	195	1.25
C6L	3.41	237	FD	Yes	1.4 $\epsilon_y$	0	195	1.21
A7L	2.93	302	SH	No	5.0 $\epsilon_y$	5	239	1.26
B7L	2.56	365	SS	No	5.0 $\epsilon_y$	4	239	1.53
C7L	2.56	351	SS	No	5.0 $\epsilon_y$	3	239	1.47
A7D	2.56	370	SW	Yes	5.0 $\epsilon_y$	3	293	1.26
B7D	2.56	416	SW	Yes	5.0 $\epsilon_y$	5	293	1.42
C7D	2.56	414	FF	Yes	5.0 $\epsilon_y$	3	293	1.41

Notes: Specimen name of form \$#%, where: \$ is A for Utelite, B for Haydite, or C for Stalite; # is girder design; % is D for dead end or L for live end. Failure modes of the form &@, where: & is F for flexural or S for shear failure; @ is D for deck crushing, F for FRP disbond, H for horizontal shear failure, S for shear failure at support, or W for web crushing from shear. No. > 3 $\epsilon_y$  is the number of stirrups with at least one strain gage measuring greater than three times the yield strain.

Four LVDTs mounted to the top and bottom flanges were used to measure girder curvature between the deck reaction points. At the girder ends, LVDTs were attached to strands on the bottom row to measure any slip between the strands and the end of the girder.

Strain in the transverse reinforcement and strain in the end region reinforcement was measured using electric resistance strain gages (ERS). ERSs were also used to measure the strain on the top surface of the deck between the deck loading points, and the strain near the ends of the FRP layers bonded to the bottom flange.

Average concrete strain over several cracks was measured using two LVDT rosettes mounted to the web near the critical section for shear. A rosette consisted of three LVDTs oriented to measure the displacement in the horizontal, vertical, and diagonal (45 degrees) directions. ERSs only measure the local strain on a stirrup and will measure much larger strains when a crack opens near the gage. An LVDT measuring the

displacement across several cracks measures an average strain and can be used to calculate the angle of inclination of the diagonal compressive stresses.

Table 5 Summary of Test Results – AASHTO/PCI BT-54 Girders

Test	a / d <sub>v</sub>	V <sub>test</sub> , kips	Failure Modes	FRP	Stirrup Strain		V <sub>LRFD</sub> , kips	$\frac{V_{test}}{V_{LRFD}}$
					Max.	No. > 3 $\epsilon_y$		
A8D	3.02	274	ST	Yes	5.0 $\epsilon_y$	2	209	1.31
B8D	3.02	277	ST	Yes	5.0 $\epsilon_y$	4	209	1.32
C8D	3.02	248	SW	Yes	5.0 $\epsilon_y$	4	209	1.19
A8L	3.02	296	ST	Yes	5.0 $\epsilon_y$	8	235	1.26
B8L	3.02	289	FF	Yes	5.0 $\epsilon_y$	5	235	1.23
C8L	3.02	288	SW	Yes	5.0 $\epsilon_y$	7	235	1.22
A9L	3.28	458	SS	Yes	5.0 $\epsilon_y$	6	385	1.19
B9L	3.28	458	FD	Yes	5.0 $\epsilon_y$	3	385	1.19
C9L	3.28	440	FF	Yes	5.0 $\epsilon_y$	6	385	1.14
A9D	3.28	462	FF	Yes	5.0 $\epsilon_y$	4	431	1.07
B9D	3.28	458	FD	Yes	3.0 $\epsilon_y$	0	431	1.06
C9D	3.28	448	FD	Yes	4.0 $\epsilon_y$	2	431	1.04

Notes: Specimen name of form \$#%, where: \$ is A for Utelite, B for Haydite, or C for Stalite; # is girder design; % is D for dead end or L for live end. Failure modes of the form &@, where: & is F for flexural or S for shear failure; @ is D for deck crushing, F for FRP disbond, S for shear failure at support, W for web crushing from shear, or T for rebar rupture. No. > 3 $\epsilon_y$  is the number of stirrups with at least one strain gage measuring greater than three times the yield strain.

A non-contact laser tracking system (FARO) was also used to measure average concrete strain. A laser from the FARO tracker followed the triple-mirror prism in a spherical steel ball. The ball was then placed in multiple targets mounted to the surface of the girder web and bottom flange. The FARO was used to record the three dimensional position of all the targets at various loading increments. The change in position of adjacent targets was used to calculate the average strain. The FARO measurements were repeatable to around 0.0010 inches which corresponds to less than 100 microstrain when the targets are spaced 12 inches apart.

## TEST PROCEDURE

Each test began in load control with the jack force increased in 5 kip increments up to about 80% of the load expected to cause web-shear cracking. Then the load increment was reduced to 2 kips until web shear cracking occurred. The loading was paused at web-shear cracking in order to mark cracks, take photographs, measure deflections using the taut-line system, measure crack widths at the mid-height of the web, and take FARO measurements. After web-shear cracking, the loading was continued in 5-kip increments. The loading was paused four or five times to take measurements and photographs. The load increment after flexural cracking occurred was also recorded. At 80% of the expected failure load, the loading was switched to displacement-control and the girder

was ramped to failure in increments of 0.25 to 0.45 inches corresponding to a load rate of 2-3 kips per 20 seconds. Flexural-shear cracking typically occurred at much higher loading increments, during the ramp to failure, so the test was not stopped to record these values.

## TEST RESULTS AND DISCUSSION

The maximum applied shear force in the test region and the failure mode of each test are given in Table 4 for the Type II girders and in Table 5 for the BT-54 girders. The first girder tested, A7D, failed in horizontal shear through the concrete deck. Of the remaining tests on Type II girders, four failed in shear and 13 failed in flexure. Six of the tests on BT-54 girders failed in shear, and the remaining six failed in flexure.

After the first test failed in horizontal shear (failure type SH in Table 4), the decks of all subsequent tests were strengthened to resist horizontal shear throughout the test region by installing concrete wedge anchors through the deck. The holes for the anchors were drilled through the deck so the anchor could be mounted into the top flange of the girders.

Three different types of shear failures were experienced in the tests: concrete crushing over a large region of the web (SW), concrete crushing near the support (SS), and rupture of the stirrups (ST). In each test resulting in a shear failure there was significant yielding in several of the stirrups as indicated by measured strains greater than three times the yield strain ( $\epsilon_y$ ). Two of the Type II girder tests that failed in shear experienced concrete crushing in the web over much of the test region (SW). The other two Type II girders failing in shear had concrete crushing as the diagonal compression was funneled to the support (SS). An example of this kind of failure is shown in Fig. 4 for the test on C7L. Three of the BT-54 girders tests failed in shear after multiple stirrups ruptured (ST). Two of the tests on BT-54 girders failed in shear after experiencing general yielding in the stirrups followed by local crushing in the web (SW). This kind of failure is shown in Fig. 3 and Fig. 5 for the tests on C8D and C8L. The failure of Test A9L is shown in Fig. 6 and was due to concrete crushing as the diagonal compression was funneled to the support (SS).

The flexural failures were caused by crushing of the deck (failure type FD) or by loss of resistance in the FRP (FF). The loss of resistance in the FRP was due to the FRP at the end of a layer debonding from the concrete substrate, or the FRP causing the concrete substrate to peel away from the bottom layer of strands. Five of the tests on Type II girders and three of the tests on BT-54 girders failed after the deck concrete crushed (FD). The flexural failure was initiated by loss of resistance in the FRP in eight of the tests on Type II girders and three of the tests on BT-54 girders. All flexural failures occurred at a maximum applied shear that was greater than the predicted shear resistance.

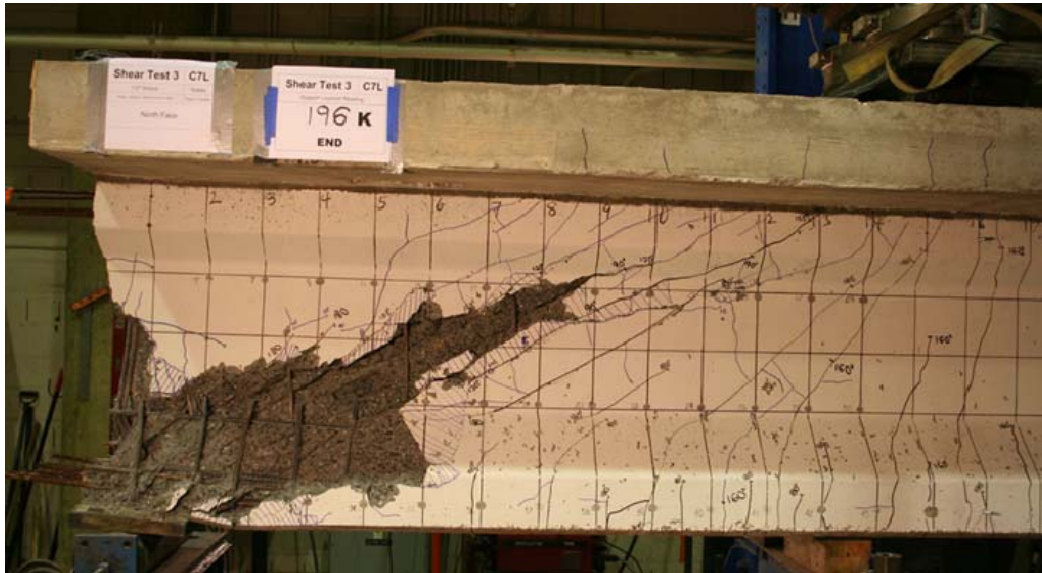


Fig. 4 Shear Failure of Girder End C7L (Type SS)



Fig. 5 Shear Failure of Girder End C8L (Type SW)

#### COMPARISON OF MEASURED AND CALCULATED SHEAR RESISTANCE

The maximum applied shear at failure ( $V_{test}$ ) was compared to the shear resistance ( $V_n$ ) calculated using the sectional design model given by the provisions of Article 5.8.3 in the AASHTO LRFD Specifications and shown in Equation (1). This model is based on MCFT which assumes that a portion of the shear resistance is carried by concrete acting in tension, as quantified by the  $V_c$  term in Equation (1). Equation (2) shows the expression for  $V_c$ , where the ability of the concrete to transmit shear is quantified by  $\beta$ . MCFT considers  $\beta$  to be reduced by longitudinal tensile strain in the web. The portion of the shear resistance carried by the transverse reinforcement ( $V_s$ ) as stirrups is given by Equation (3). The angle of inclination of the diagonal cracks ( $\theta$ ) determines the number

of stirrups that contribute to the shear resistance. MCFT also considers  $\theta$  to be dependent on the longitudinal strain in the web. The 2004 version of the AASHTO LRFD Specifications gave tables to calculate  $\beta$  and  $\theta$  using an iterative method. The current version of the AASHTO LRFD Specifications uses a simplified method to directly calculate  $\beta$  and  $\theta$  without iteration.

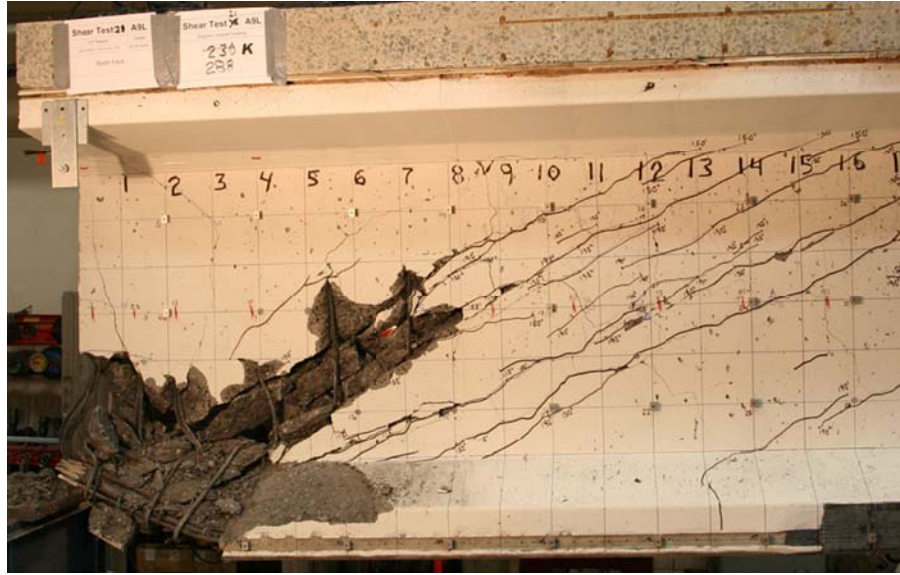


Fig. 6 Shear Failure of Girder End A9L (Type SS)

$$V_n = V_c + V_s + V_p \leq 0.25f'_c b_v d_v + V_p \quad (1)$$

$$V_c = 0.0316\beta\sqrt{f'_c} b_v d_v \quad \text{where } f'_c \text{ is in ksi units} \quad (2)$$

$$V_s = \frac{A_v f_y d_v \cot \theta}{s} \quad (3)$$

The shear resistance for a girder test was calculated using the iterative method of the 2004 AASHTO LRFD Specifications at the critical section for shear as specified by Article 5.8.3.2. The critical section occurs at a distance equal to  $d_v$  from the edge of the bearing plate over the rolling support. For the preliminary estimate of the shear resistance in this paper,  $f'_c$  was taken as 10 ksi for all girders, and the yield strength of the stirrups was taken as 72 ksi, which was measured through tension tests of stirrup samples using the 0.2% offset method. Also, no modification for lightweight concrete was used in the calculation of  $V_c$  and the  $\phi$  factor was not used to reduce  $V_n$  ( $\phi = 1$ ). The shear resistance calculated for each girder test ( $V_{LRFD}$ ) and the shear strength ratios ( $V_{test}/V_{LRFD}$ ) are shown in Table 4 and Table 5 for the Type II girders and BT-54 girders.

The shear strength was conservatively predicted for all the girders. The shear strength ratios ranged between 1.19 and 1.53 and had a mean of 1.32 with a coefficient of variation (COV) of 9.1%. The mean shear strength ratios of all the girder tests ending in a shear failure are shown in Table 6.

## EFFECT OF TRANSVERSE REINFORCEMENT AREA

The effect that the amount of transverse reinforcement had on the shear strength ratio is shown in Fig. 7. The amount of transverse reinforcement is shown as the shear reinforcement ratio ( $\rho_v$ ) multiplied by the yield stress in the reinforcement ( $f_y$ ). The results from the tests on girders with draped strands are not shown because all six tests ended in flexural failures. Table 4 and Table 5 also show the shear strength ratio for each girder test.

The six tests on Girder Design 5 with a low amount of transverse reinforcement and 12 prestressing strands all ended in a flexural failure; however they all had at least one stirrup with a measured strain greater than  $3\epsilon_y$ . Five out of six tests on Girder Design 7 with a moderate amount of transverse reinforcement and 22 prestressing strands ended in a shear failure, and all six tests had at least three stirrups with a measured strain greater than  $3\epsilon_y$ . By comparing the shear strength ratios for the three tests on 5D (mean of 1.47) with 5L (mean of 1.35) and the shear strength ratios of 7L (mean of 1.42) with 7D (mean of 1.36), there appears to be a decrease in conservatism of the shear resistance predicted by the AASHTO LRFD Specifications as the amount of transverse reinforcement increases for a given number of prestressing strand. Stated another way, the level of conservatism appears higher in girder tests with smaller amounts of transverse reinforcement. However, when comparing shear strength ratios of all twelve tests on girder designs 5 and 7, an overall trend is not as clear.

Table 6 Mean Shear Strength Ratio by Concrete Mix and Girder Size

Girder Size	Mean Shear Strength Ratio $\frac{V_{test}}{V_{LRFD}}$			
	Utelite	Haydite	Stalite	All Mixes
Type II Girders	1.26	1.47	1.47	1.42
BT-54 Girders	1.25	1.32	1.20	1.25
All Girders	1.25	1.42	1.29	1.32

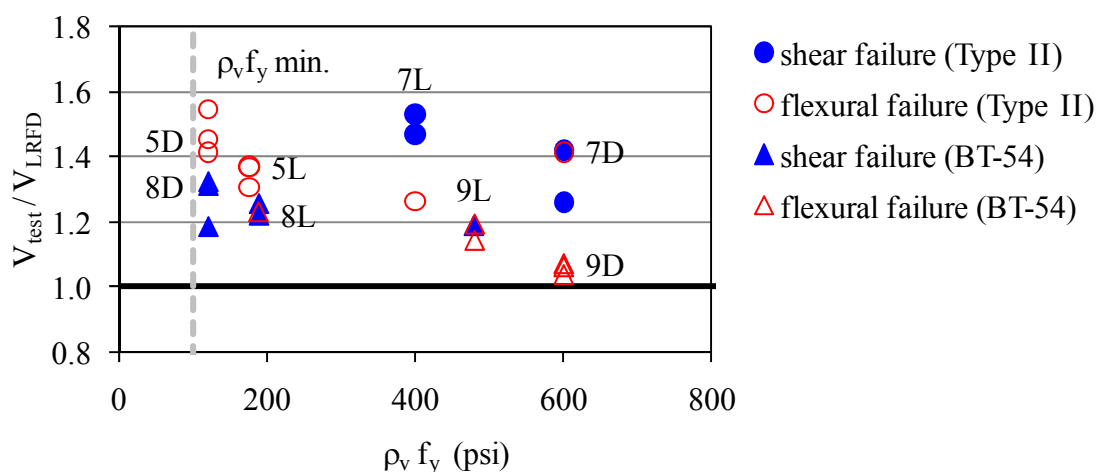


Fig. 7 Nominal Shear Resistance Ratio versus Transverse Reinforcement Ratio

Girder Design 8 was a BT-54 girder with a low amount of transverse reinforcement and all tests except one ended in a shear failure. All six tests had at least two stirrups with measured strains greater than  $3\epsilon_y$ . A similar trend of a decrease in conservatism of the shear resistance predicted by the AASHTO LRFD Specifications as the amount of transverse reinforcement increases can also be seen by comparing the shear strength ratio for 8D (mean of 1.27) with 8L (mean of 1.24) in Fig. 7. This trend has also been observed in tests on normal weight prestressed girders<sup>2</sup>.

A more noticeable difference can be seen by comparing the shear strength ratio from tests of AASHTO Type II girders (36 inch girder depth) with the tests on AASHTO/PCI BT-54 girders (54 inch girder depth) that have a similar amount of transverse reinforcement. The average shear resistance ratio for 5D is 16% greater than for 8D, 5L is 9% greater than 8L, and 7L is 21% greater than 9L. 7D is not compared to 9D because none of the tests on end 9D ended in a shear failure.

#### AASHTO LRFD SPECIFICATIONS FOR LWHPC

This section will address the provisions of the AASHTO LRFD Specifications that relate specifically to lightweight concrete. The provisions include the modification factor for lightweight concrete, web-shear cracking, minimum transverse reinforcement, and maximum shear stress for used of the sectional design model.

The measured concrete properties  $f'_c$  and  $f_{ct}$  at the time the girder was tested are shown in Table 7. for the Type II and BT-54 girders. The table also shows the splitting ratio ( $f_{ct}/\sqrt{f'_c}$ ) for each girder, which is incorporated into the modification factor for lightweight concrete. Table 8 gives the mean splitting ratios by aggregate source and girder size. The mean splitting ratio ranged from 6.94 to 7.56 for the different aggregate sources. Also, the splitting ratio for the concrete in the BT-54 girders was 11% higher than for the concrete in the Type II girders.

The web-shear cracking strength is predicted by  $V_{cw}$  given in Article 5.8.3.4.3 and is shown in Equation (4). A similar expression for  $V_{cw}$  was originally in the AASHTO Standard Specification, but was modified by the results of NCHRP project 12-56 to extend the applicability of the expression to both prestressed and nonprestressed members<sup>11</sup>.



Table 7 Girder Concrete Properties and Cracking Results

Test Name	$f'_c$ , ksi	$f_{ct}$ , ksi	$\frac{f_{ct}}{\sqrt{f'_c}}$	$V_{Crack}$	$V_{cw}$	$\frac{V_{Crack}}{V_{cw}}$
A5	10.55	0.76	7.43	129	87.2	1.48
B5	10.38	0.74	7.29	134	87.2	1.54
C5	11.25	0.75	7.03	134	87.2	1.54
A6	8.79	0.72	7.72	160	104.0	1.53
B6	9.57	0.74	7.61	187	104.0	1.80
C6	9.86	0.72	7.30	167	104.0	1.60
A7	9.22	0.82	8.50	176	111.0	1.58
B7	10.37	0.79	7.77	186	111.0	1.67
C7	10.34	0.72	7.12	176	111.0	1.59
A8	11.24	0.76	7.21	145	116.3	1.24
B8	11.94	0.78	7.12	180	116.3	1.54
C8	11.62	0.73	6.78	159	116.3	1.37
A9	10.81	0.72	6.92	187	139.0	1.35
B9	10.95	0.80	7.66	227	139.0	1.63
C9	10.37	0.66	6.47	202	139.0	1.45

Notes: Specimen name of form \$#, where: \$ is A for Utelite, B for Haydite, or C for Stalite; # is girder design

Table 8 Mean Splitting Ratio by Concrete Mix and Girder Size

Girder Size	Mean Splitting Ratio $\frac{f_{ct}}{\sqrt{f'_c}}$			
	Utelite	Haydite	Stalite	All Mixes
Type II Girders	7.88	7.55	7.15	7.53
BT-54 Girders	7.07	7.39	6.62	7.03
All Girders	7.56	7.49	6.94	7.33

$$V_{cw} = (0.06\sqrt{f'_c} + 0.30f_{pc})b_v d_v + V_p \quad \text{where } f'_c \text{ is in ksi units} \quad (4)$$

The initiation of web-shear cracking in the Type II girder was more difficult to detect than in the BT-54 girders. At the initiation of the first web-shear crack in tests of Type II girders, the cracks were typically fewer in number and more narrow in width than web-shear cracks in tests of BT-54 girders. Web-shear cracking in the BT-54 girder tests was associated with loud “pops” as multiple cracks quickly opened between the top and bottom flanges.

Web-shear cracking ( $V_{crack}$ ) was the average of the applied shear in girder tests at each end at the initiation of the first web-shear crack. Table 7 gives  $V_{crack}$ ,  $V_{cw}$ , and the web-shear cracking strength ratios ( $V_{crack}/V_{cw}$ ) for the girders. The mean cracking strength ratios of all the girders are shown in Table 9 by aggregate source and girder size. The



web-shear cracking strength was conservatively predicted for all the girders. The mean cracking strength ratio was 1.53 with a COV of 9.0% for all the girders.

Table 9 Mean Web-Shear Cracking Strength Ratio by Concrete Mix and Girder Size

Girder Size	Mean Web-Shear Cracking Strength Ratio $\frac{V_{Crack}}{V_{cw}}$			
	Utelite	Haydite	Stalite	All Mixes
Type II Girders	1.53	1.74	1.60	1.59
BT-54 Girders	1.30	1.59	1.41	1.43
All Girders	1.44	1.64	1.51	1.53

The mean cracking strength ratio for the Type II girders was 11% higher than for the BT-54 girders. This appears consistent with a typical size effect where the strength of a section in shear tends to decrease with the depth of a section. However, the increase in cracking strength for the Type II girders can mostly be explained by their 7% higher mean splitting ratio.

The cracking strength ratio is shown versus the splitting ratio in Fig. 8. Splitting ratios greater than 6.7 do not require modification of the  $\sqrt{f'_c}$  term ( $\lambda = 1$ ) for lightweight concrete. The only girder with a splitting ratio less than 6.7 still had a cracking strength ratio of 1.45. The cracking strength ratio versus  $\sqrt{f'_c}$  is shown in Fig. 9. Recall that when  $f_{ct}$  is not specified, the  $\sqrt{f'_c}$  term is specified to be multiplied by 0.75 for an all lightweight concrete and 0.85 for a sand lightweight concrete, implying that the cracking strength is directly related to  $\sqrt{f'_c}$ .

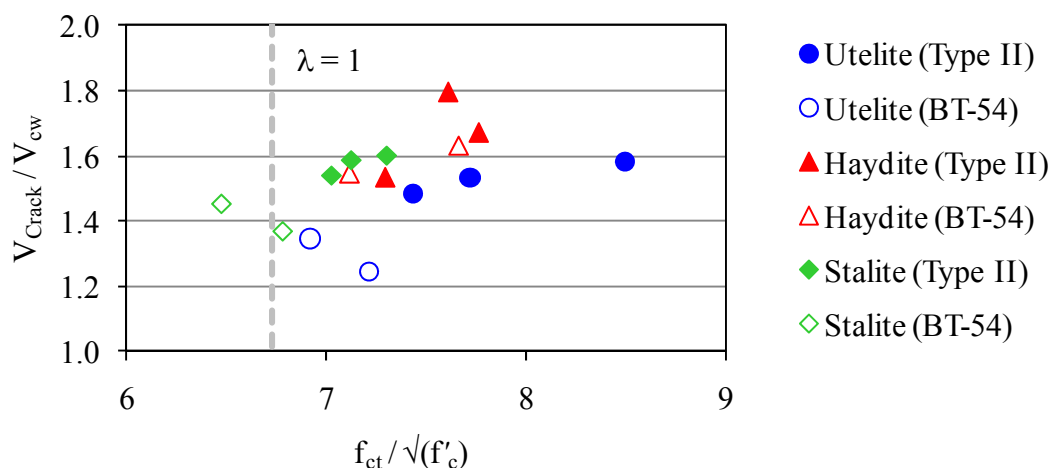


Fig. 8 Web-Shear Cracking Strength Ratio versus Splitting Ratio

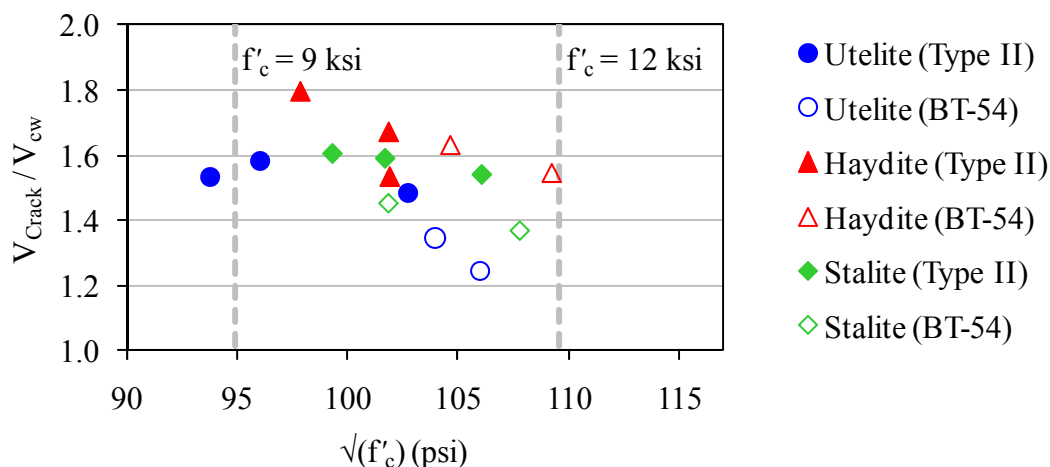


Fig. 9 Web-Shear Cracking Ratio versus  $\sqrt{f'_c}$

A comparison of Fig. 8 and Fig. 9 shows that  $f_{ct}$  is a better indicator of the web cracking strength than  $\sqrt{f'_c}$ . The relative position of points in Fig. 8 and Fig. 9 are very different. For example, the three data points for the Type II girders made with Utelite, are on the right side of Fig. 8 indicating a greater splitting ratio than many of the other data points. However these same data points in Fig. 9 are on the left side, indicating a lower  $\sqrt{f'_c}$  than many of the data points. Additional evidence comes from the slight upward trend in the data of Fig. 8 indicating that the cracking strength ratio increases with the splitting ratio. However, a downward trend is shown in Fig. 9 where the cracking strength ratio decreases with an increase in  $\sqrt{f'_c}$ . As shown by the lines in Fig. 9, this data represents a limited range of compressive strengths, between around 9 ksi and 12 ksi.

The splitting ratio also correlates well with the shear resistance for girders with shear reinforcement, although not as well as with web-shear cracking. Concrete mixes with a slightly higher or lower splitting ratio did have a proportionally higher or lower shear strength, respectively. Although the Utelite mix, with the lowest mean shear strength ratio also had the highest tensile strength ratio. The mean splitting ratio of the Type II girders was 7% higher than for the BT-54 girders and the mean shear strength ratio of the Type II girders was 14% higher. This difference may be due in part to the size effect discussed previously in this paper.

A minimum amount of transverse reinforcement is required for post-cracking ductility. Equation (5) gives the expression in the AASHTO LRFD Specifications for the minimum shear reinforcement. Tests completed at Purdue<sup>12</sup> involving two high-strength sand-lightweight prestressed girders with the minimum amount of transverse reinforcement failed in shear at nearly the same force but had  $f'_c$  of 6.5 ksi and 10.1 ksi. The shear strength ratios for the two tests were 1.20 and 1.08, respectively. The authors concluded that because the shear force at failure did not increase with  $\sqrt{f'_c}$ , the requirements for minimum reinforcement in the AASHTO LRFD Specifications were not as conservative for high-strength girders.

$$A_v = 0.0316 \sqrt{f'_c} \frac{b_v s}{f_y} \quad \text{where } f'_c \text{ is in ksi units} \quad (5)$$

In regards to the shear performance of specified density LWHPC near the minimum amount of reinforcement, Fig. 7 shows that the shear strength ratio for girder end 5D and 8D were all conservative and ranged from 1.19 to 1.55. The reserve shear capacity beyond web-cracking is an estimate of post-cracking ductility and is given by the ratio of  $V_{\text{test}}$  to  $V_{\text{crack}}$ . The  $V_{\text{test}}/V_{\text{crack}}$  ratios for the six tests on ends 5D and 8D ranged from 1.44 to 1.93 with mean of 1.63. The specified density girders with minimum reinforcement tested in this research program gave consistently higher shear strength ratios than the girder in the Purdue study with similar  $f'_c$ .

The effect the maximum shear stress ( $v_u$ ) has on the shear strength ratio is shown in Fig. 10. Equation (6) gives the expression for  $v_u$  and is based on Article 5.8.2.9 in the AASHTO LRFD Specifications. The  $\sqrt{f'_c}$  from the time the girder was tested is used to normalize  $v_u$ . Four tests reached a  $v_u/f'_c$  between 0.18 and 0.20 (A7D, B7D, B7L, and C7D) and all attained shear strength ratios of at least 1.26 and had significant yielding ( $>3\varepsilon_y$ ) measured in at least three stirrups. The test on B7L had local crushing near the supports, but achieved a shear strength ratio of 1.53 with significant yielding in four of its stirrups. This shows that using the sectional model up to the limit of  $0.18f'_c$  on  $v_u$  allowed the stirrups to yield before local crushing near the supports. None of the tests reached a shear stress of near  $0.25f'_c$ , so the maximum shear stress limit cannot be evaluated.

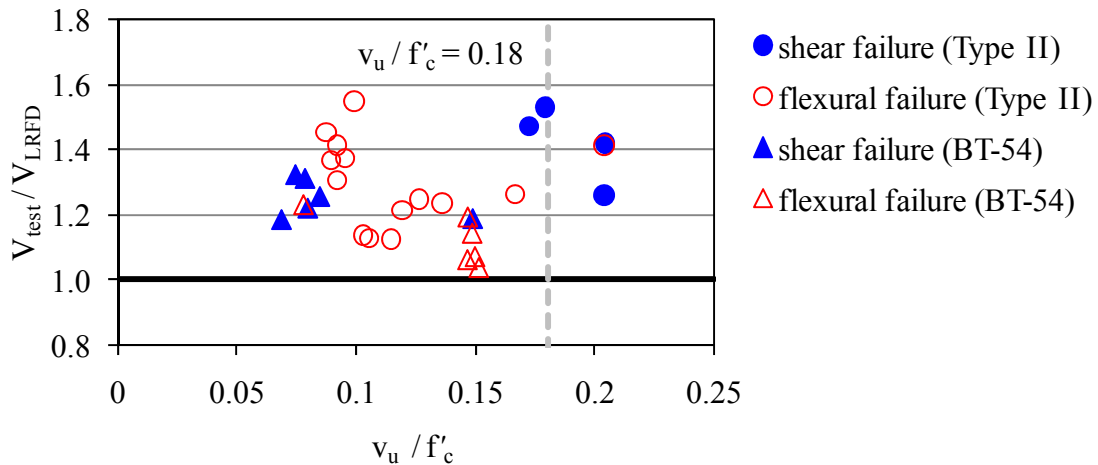


Fig. 10 Nominal Shear Resistance Ratio versus Normalized Maximum Shear Stress

$$v_u = \left( \frac{V_{\text{test}} - V_p}{b_v d_v} \right) \quad (6)$$

## PRELIMINARY CONCLUSIONS

This paper gave the results for 30 shear tests on specified density LWHPC prestressed girders. All girders had at least the minimum transverse reinforcement required by the AASHTO LRFD Specifications. The cylinder compressive strengths of the girders at the time of test ranged from 8.8 to 11.9 ksi. The following preliminary conclusions can be made based on the shear tests that were part of this study:

1. The sectional method in the AASHTO LRFD Specifications provided conservative predictions of the shear resistance of all the tests ending in shear failure.
2. For girders with the same number of prestressing strands, the level of conservatism provided by the shear provisions in the AASHTO LRFD Specifications was higher in girder tests with smaller amounts of transverse reinforcement.
3. The level of conservatism provided by the shear provisions in the AASHTO LRFD Specifications was less for the girders with greater depth.
4. The web-shear cracking strength was conservatively predicted by  $V_{cw}$  which is part of the Simplified Procedure for shear resistance in the AASHTO LRFD Specifications.
5. The splitting tensile strength gave a much stronger correlation with the web-shear cracking strength than did  $\sqrt{f'_c}$ . The splitting tensile strength also correlated reasonably well with overall shear resistance.
6. The girders with the minimum amount of transverse reinforcement required by the AASHTO LRFD Specifications had considerable post-cracking strength. Also, the maximum applied shear was considerably higher than the shear resistance predicted by AASHTO LRFD Specifications.
7. The stirrups yielded before local crushing occurred near the supports in the four tests that reached the  $0.18f'_c$  limit on average web shear stress. This supports the use of the  $0.18f'_c$  limit in the AASHTO LRFD Specifications for the use of the sectional design method.

## ACKNOWLEDGEMENTS

The publication of this article does not necessarily indicate approval or endorsement of the findings, opinions, conclusions, or recommendations either inferred or specifically expressed herein by FHWA or the United States Government. This paper was created by PSI on behalf of FHWA as part of contract DTFH61-10-D-00017.

The authors would like to acknowledge the hard work of the following members of the Structures Lab technician staff at TFHRC who have worked diligently to construct, instrument, and test the shear girders: Marshall Davis, Kevin Deasy, Paul Ryberg, Brian Story, and Tim Tuggle.

## NOTATION

$a$	= shear span
$A_v$	= area of transverse reinforcement
$b_v$	= effective web width
$d_v$	= effective depth for shear
$f'_c$	= concrete compressive strength per ASTM C39
$f_{ct}$	= concrete splitting tensile strength per ASTM C496
$f_{pc}$	= compressive stress in concrete at cross-section centroid after all prestress losses have occurred
$f_y$	= transverse reinforcement yield strength
$s$	= spacing of transverse reinforcement
$V_c, V_s, V_p$	= components of $V_n$ provided by concrete, transverse reinforcement, and prestressing force
$V_{Crack}$	= applied shear in the test region at initiation of web-shear cracking
$V_{ci}, V_{cw}$	= shear at flexural-shear cracking, shear at web-shear cracking
$V_{LRFD}$	= calculated shear resistance at the critical section using the sectional design method in the AASHTO LRFD Specifications
$V_n$	= nominal shear resistance
$V_{test}$	= maximum applied shear for in the test region
$v_u$	= average shear stress in the effective web
$\beta$	= factor indicating ability of diagonally cracked concrete to transmit shear in MCFT
$\epsilon_y$	= transverse reinforcement yield strain
$\lambda$	= modification factor lightweight concrete in ACI-318 Building Code
$\theta$	= inclination angle of diagonal compressive stresses in MCFT
$\rho_v$	= transverse reinforcement ratio, $A_v/(b_v s)$

## REFERENCES

1. AASHTO, "AASHTO LRFD Bridge Design Specifications: Customary U.S. Units," American Association of State Highway and Transportation Officials, 3th Edition, 2004.
2. Hawkins, N. M., and Kuchma, D. A., "Application of LRFD Bridge Design Specifications to High-Strength Structural Concrete: Shear Provisions," *NCHRP Report 579*, National Cooperative Highway Research Program, Transportation Research Board, 2007, 206 pp.
3. ACI Committee 213, "Guide for Structural Lightweight Aggregate Concrete," ACI 213R-03, American Concrete Institute Committee 213, Farmington Hills, MI., 2003.

4. Ivey, D. L. and Buth, E., "Shear Capacity of Lightweight Concrete Beams," *ACI Journal*, October 1967, pp. 634-643.
5. Dymond, B. Z., Roberts-Wollman, C. L., and Cousins, T. E., "Shear Strength of a PCBT-53 Girder Fabricated with Lightweight Self-Consolidating Concrete," Virginia Transportation Research Council, Charlottesville, VA, 2007, 74 pp.
6. Meyer, K. F., and Khan, L. F., "Shear Behavior of Pretensioned Girders Constructed with Slate High Strength Lightweight Concrete," *Proceedings of the 2004 PCI National Bridge Conference: Bridges for Life*, Atlanta, GA, Oct. 17-20, 2004.
7. Salandra, M. A. and Ahmad, S. H., "Shear Capacity of Reinforced Lightweight High-Strength Concrete Beams," *ACI Structural Journal*, V. 86, No. 6, Nov.-Dec. 1989, pp. 697-704.
8. AASHTO, "AASHTO LRFD Bridge Design Specifications: Customary U.S. Units," American Association of State Highway and Transportation Officials, 5th Edition, 2010.
9. ACI Committee 318, "Building Code Requirements for Structural Concrete (ACI 318-08) and Commentary," American Concrete Institute, Farmington Hills, MI, 2008.
10. Vecchio, F. J. and Collins, M. P., "The Modified compression Field Theory for Reinforced Concrete Elements Subjected to Shear," *ACI Journal*, V. 83, No. 2, Mar. 1986, pp. 219-231.
11. Kuchma, D., Kim, K. S., Nagle, T. J., Sun, S., and Hawkins, N. M., "Shear Tests on High-Strength Prestressed Bulb-Tee Girders: Strengths and Key Observations," *ACI Structural Journal*, V. 105, No. 3, May-June 2008, pp. 358-367.
12. Ramirez, J. A., Olek, J., Rolle, E., and Malone, B., "Performance of Bridge Decks and Girders with Lightweight Aggregate Concrete," Joint Highway Research Program, Purdue University, West Lafayette, IN, 2000, 616 pp.